Electronic Supplementary Information for:

Hierarchical Micro/Nano Porous Silicon Li-ion Battery Anode

Yu Zhao,[a] Xizheng Liu,[a] Huiqiao Li,[a] Tianyou Zhai,[b] and Haoshen Zhou[a]*

[a] *Energy Interface Research Group, National Institute of Advanced Industrial Science and Technology (AIST), Umezono 1-1-1, Tsukuba 305-8568, Ibaraki, Japan. E-mail: hs.zhou@aist.go.jp*

[b] *Inorganic Nanostructured Materials Group, National Institute for Materials Science (NIMS), Namiki 1-1, Tsukuba 305-0044, Ibaraki, Japan.*

S1. Experimental details.

Synthesis of porous silicon powder. In a typical procedure, silicon wafer (50±0.5 mm in diameter and 280±20 μm in thickness, boron-doped, 0.001–0.003 Ω·cm, Semitec Corp.) was cleaned follow the standard procedure and smashed into silicon powder by mechanical milling. The silicon powder (0.05 mol) was then dispersed in 50 mL $AgNO_3$ solution (0.05 M, Wako) followed by adding 10 mL HF (5 M) with stirring. After stirred for 5 min, the precipitate composed of Ag-decorated silicon powder was washed with distilled water for several times before etching. The etching of silicon powder followed the wet-chemical etching method.[13] The etchant was comprised of an distilled water/ethanol (4:1 v:v) solution of 5 M HF (Wako) and 0.12 M H_2O_2 (Wako). The mixture was left to soak at room temperature for 4 h. The obtained powder was washed with deionized water, and soaked in diluted nitric acid (Wako) for 30 min to remove the silver composition.

Synthesis of carbon-coated porous silicon powder. The porous silicon powder was dispersed in 20 mL carbon-gel of neutral *p*H value prepared by mixing resorcinol (0.05 M, Wako) and formaldehyde (0.1 M, 5–10% methanol stabilized, Wako). The mixture was kept at 60 °C for 30 min and then 85 °C for 6 h. The resulting phenolic resin/silicon composites were washed with distilled water and sintered at 850 °C for 3 h under constant H_2/argon flow (4% H_2) to form a carbon-coating on the porous silicon powder. The content of carbon composition can be well controlled by controlling the concentration of carbon-gel, and can be calculated by the weight of product after and before sintering. In our experiment, the content of carbon composition is about 9.2% in the total weight the obtained product.

Fabrication of porous silicon powder anodes. The electrodes were made by mixing the active materials with conductive carbon black and polytetrafluoroethylene with mass ratio of 75: 20: 5 for porous silicon powder and 85: 10: 5 for carbon-coated porous silicon powder, respectively. The above mixtures were severally spread with a typical size of 10 mm in diameter and pressed onto a copper mesh as current collector. The loading amount of the active materials is *c.a.* 6 mg/cm^2. The electrodes were dried at 85 °C overnight in vacuum prior to cell assembly. Then CR2032 coin cells were assembled in an Argon-filled glove box using the as-prepared anodes as working electrodes and lithium metal foil as counter electrodes. Celgard 2325 was used as a separator and the electrolyte was a commercial solution of 1.0 M $LiPF_6$ in 1:1 w/w ethylene carbonate: diethyl carbonate.

Characterization. The porous structure was examined by field-emission scanning electron microscopy (FE-SEM, JEOL 6700F) and high-resolution transmission electron microscopy (HRTEM, JEOL JEM-3000F). Powder X-ray diffraction (XRD) patterns were collected with a Bruker D8 Advanced Diffractometer using Cu K_α radiation. Nitrogen sorption isotherms were measured at 77 K with Micromeritics TriStar 3000. Before measurements, the samples were degassed at 80 °C for at 20 h. The specific surface area was calculated by the Brunauer–Emmett–Teller (BET) method using the adsorption branch in a relative pressure range from 0.04 to 0.2. The total pore volume (V_t) was the adsorbed amount at a P/P_0 of 0.992. The electrochemical measurements were performed on Hokudo Denko Charge/Discharge instrument. The specific capacity was based on the total mass of the working electrode.

S2. XRD measurement.

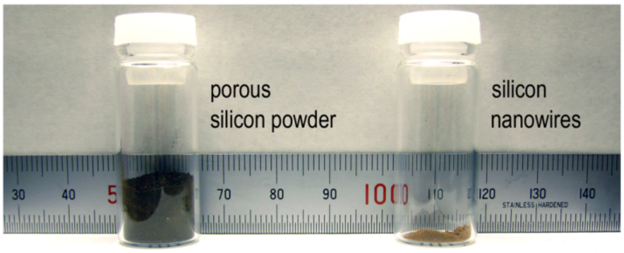

Figure S2. Digital images showing the high yield of porous silicon using silicon powder as starting material (left) compared with that collected on silicon wafer (right).

S3. XRD measurement.

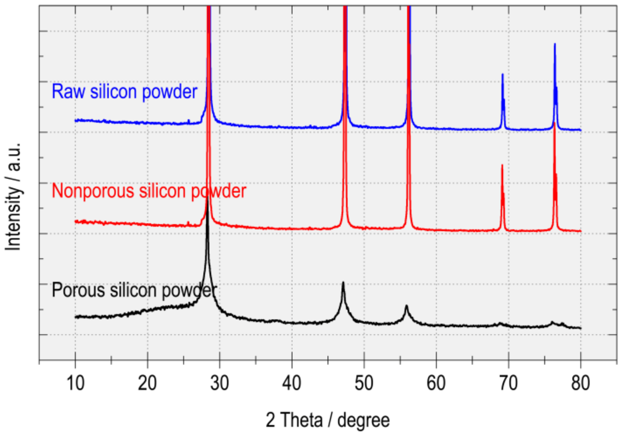

Figure S3. XRD patterns of the porous silicon powder and the reference nonporous silicon powder prepared by using silicon wafer with higher resistance (5–10 Ω•cm), and the raw silicon powders made by mechanical milling. Compared with the nonporous or raw silicon powder, the diffraction peaks of porous silicon powder were significantly broadened. According to Scherrer Equation, the mean size of the ordered crystalline domains is about 25 nm.

S4. Panoramic FESEM image of porous silicon powder.

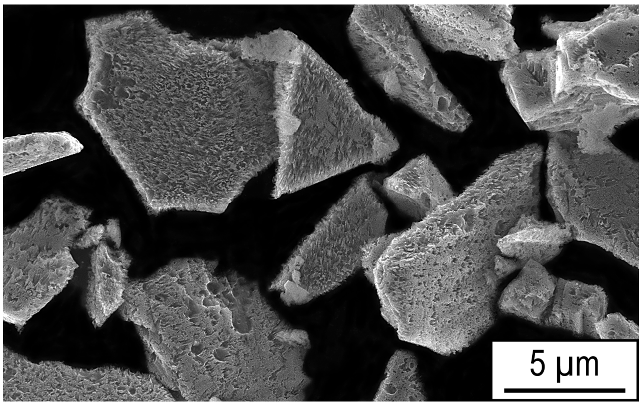

Fig. S4. Panoramic FESEM image showing the size distribution of the porous silicon powder.

S5. Internal structure of the porous silicon powder.

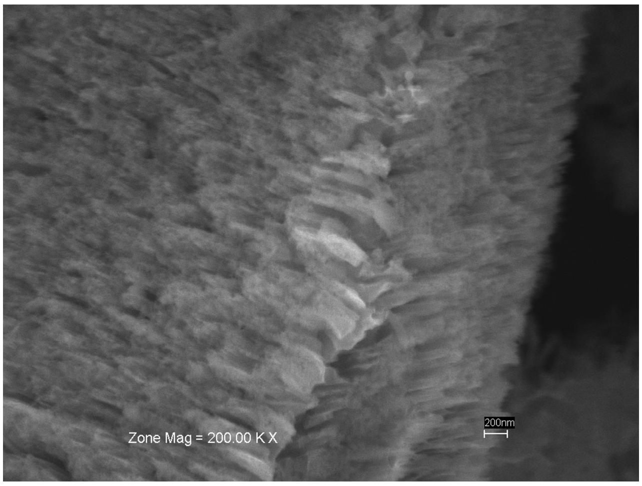

Fig. S5. FESEM image showing the internal structure of the porous silicon powder.

S6. Cyclic voltammetry profile of the porous silicon electrode.

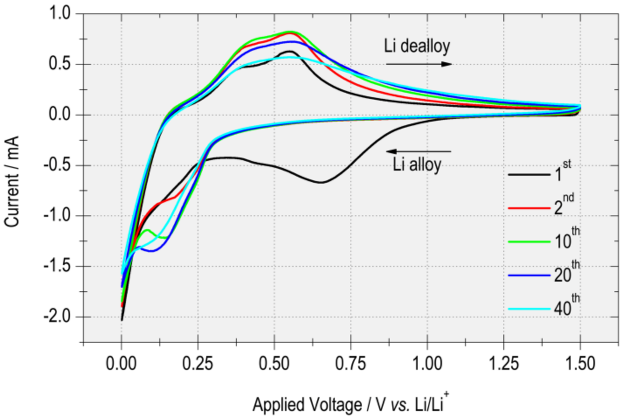

Fig. S6. The 1st, 2nd, 10th, 20th and 40th cyclic voltammogram of porous silicon electrode from 1.5 V to 0.01 V versus Li/Li$^+$ at 1 mVs^{-1} scan rate. In the first cathodic branch, the broad cathodic peak between 0.4 and 0.8 V are attributed to the formation of a solid-electrolyte interphase (SEI) passivation layer on the surface of the porous silicon electrode as a result of the reaction of lithium with electrolyte.[1] The formation of the Li–Si alloy began at a cathodic peak of 0.3 V. In the first anodic branch, the two peaks which located at 0.39 and 0.55 V and become more distinct in the following cycles correspond to de-lithiation back to amorphous Si.[2] It is expected that the rate of the reconstruction process is governed by the transport rate of lithium into crystalline silicon or the rate of amorphous Si–Li alloy formation, this kinetic bottleneck is likely to lead to the gradual activation of the porous silicon electrodes at each cyclic voltammetry cycle.

S7. **Galvanostatic charge-discharge profiles of the silicon nanoparticle electrode.**

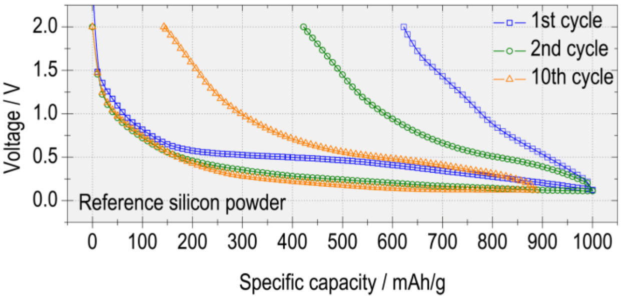

Fig. S7. Galvanostatic charge/discharge profiles of the reference silicon powder electrode at a given discharge capacity of 1000 mAhg^{-1} in the voltage range of 2–0 V.

S8. Irreversible capacity of silicon electrodes at different discharge depth.

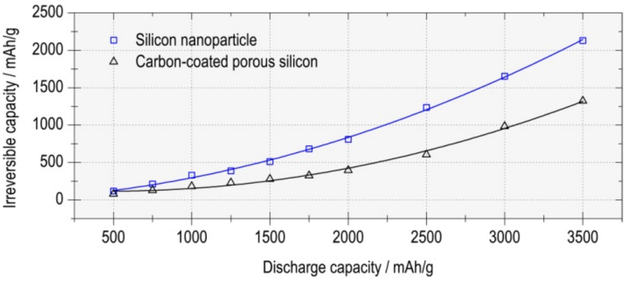

Fig. S8. Irreversible capacity *vs* discharged capacity profiles of carbon-coated porous silicon and silicon nanoparticles.

S9. Impedance response of porous silicon/Li metal and carbon-coated porous silicon/Li metal half cell.

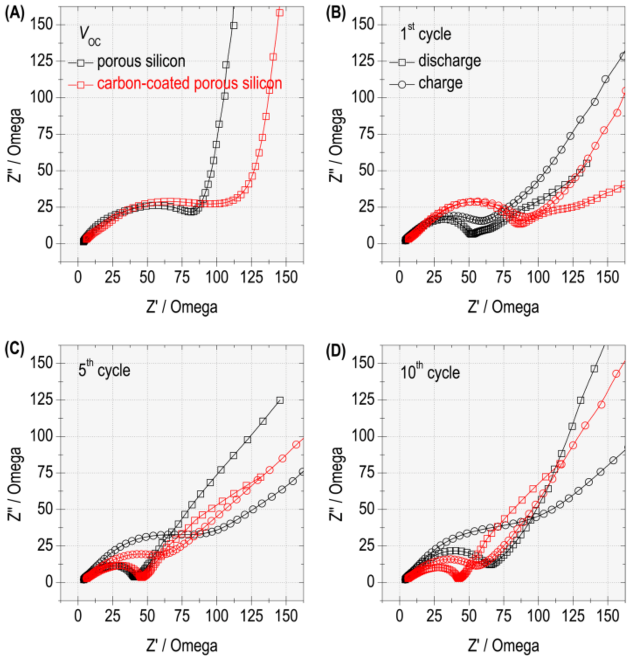

Fig. S9. Nyquist plots of porous silicon/Li metal (black) and carbon-coated porous silicon/Li metal (red) half cell. The impedance response was measured at (A) V_{OC} and (B)–(D) the end 1st, 5th and 10th charge (square)/discharge (circle) cycles. The cut-off voltage of charging is set to 2.0 V; the capacity is fixed to 1500 mAhg^{-1} when discharging. The cells were rested for a certain period of time before impedance measurement.

Fig. S9 shows the impedance response of porous silicon/Li metal and carbon-coated porous silicon/Li metal half cell measured at a given discharged capacity of 1500 mAhg^{-1} and a charged potential of 2.0 V. It is noted that the impedance decrease with the number of cycles in both cells, consistent with the result that the silicon electrode is activated for the redox reaction in the course of voltammetric cycling. The Nyquist plots at open circuit voltage (V_{OC}) shown in Figure 7A, in which the depressed semicircle can be well simulated according to the models documented elsewhere.[3] The calculated electrode resistance and grain-boundary resistance are 2.9 and 94.2 Ω for porous silicon electrode, and 3.1 and 128.4 Ω for carbon-coated porous silicon electrode. After carbon-coating, the electrode resistance shows an increase of 7%. Meanwhile, the increase of grain-boundary resistance is 36%, which mainly arise from the different ratio of conductive carbon black used in fabricating the electrode (75: 20 for porous silicon powder and 85: 10 for carbon-coated porous silicon powder). In the subsequent cycles, the typical Nyquist plots of these half cells consist of two semicircles and one 45◦ linear diffusion drift as shown in Figure 7B–7D. During the discharge state, two factors will seriously affect the total resistance of the electrode: the first is the lithium insertion will increase the conductivity of the electrode,[4] and the other is the formation of SEI layer will increase the resistance of the electrode. For the porous silicon electrode, the total resistance undergoes a gradually and a decrease process in the first 5 cycles and then an increase process in the following cycles to obtain a stable state till the 10th cycle. In other words, the conductivity increase caused by lithium insertion is dominant in the first 5 cycles, and then the conductivity decrease caused by SEI layer formation in the following several cycles until a balance is reached after the 10th cycle. For the carbon-coated porous silicon electrode, the total resistance is gradually decreased till a stable state is obtained in the 10th cycle, suggesting that the carbon coating effectively slowdown the formation of SEI layer. During the charge state, the total resistance of porous silicon electrode undergoes similar process as in the discharge state. When the surface of silicon electrode is covered with the initial SEI layer, the total resistance is abruptly decreased to the minimum value. After this, the reduction of organic solvents plays a major role in SEI layer formation and the total resistance is gradually increased with the growth of the SEI layer. This observation is in consistent with previous report.[5] In contrast, the total resistance of carbon-coated porous silicon electrode is gradually decreased till a stable state reached, which clearly demonstrated that by coating a carbon layer, the formation of SEI layer can be effectively reduced. We can attribute such a phenomenon to the masking effects from the pyrolyzed carbon layer,[6] which may fasten the Si/C interface to sustain better cyclability.

S10. Morphology changes in porous silicon powder from reaction with Li.

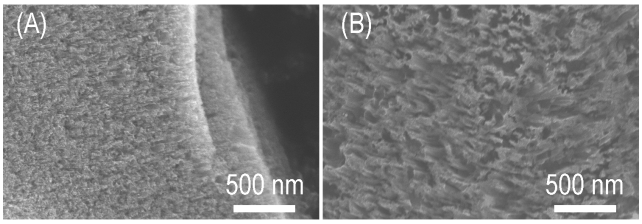

Fig. S10. SEM images of porous silicon powder (A) before and (B) after the 50th electrochemical cycling (same magnification), revealing that the porous silicon powder undergo volume expansion but no fracture or pulverization was observed.

References in Electronic Supplementary Information

1 G. X. Wang, J. H. Ahn, J. Yao, S. Bewlay and H. K. Liu, *Electrochem. Commun.* 2004, **6**, 689.
2 J. Li and J. R. Dahn, *J. Electrochem. Soc.* 2007, **154**, A156.
3 (a) R. Ruffo, S. S. Hong, C. K. Chan, R. A. Huggins and Y. Cui, *J. Phys. Chem. C* 2009, **113**, 11390. (b) W.-R. Liu, J.-H. Wang, H.-C. Wu, D.-T. Shieh, M.-H. Yang and N.-L. Wu, *J. Electrochem. Soc.* 2005, **152**, A1719.
4 E. Pollak, G. Salitra, V. Baranchugov and D. Aurbach, *J. Phys. Chem. C* 2007, **111**, 11437.
5 Y. M. Lee, J. Y. Lee, H.-T. Shim, J. K. Lee and J.-K. Park, *J. Electrochem. Soc.* 2007, **154**, A515.
6 Y. Liu, T. Matsumura, N. Imanishi, A. Hirano, T. Ichikawa and Y. Takeda, *Electrochem. Solid-State Lett.* 2005, **8**, A599.